Search of Anomalous ZZγ and Z$\gamma\gamma$ Couplings with the L3 Detector

Eusebio Sánchez Álvaro

CIEMAT (Madrid)

Abstract

The existence of anomalous ZZγ and Z$\gamma\gamma$ couplings has been studied using the L3 detector at LEP. This study uses the process $e^+e^- \rightarrow Z\gamma$ at center-of-mass energies between 161 GeV and 183 GeV. Limits at the 95% C. L. are set in the eight possible anomalous couplings. These limits are an improvement of the previous results at LEP1 due to the increase of the sensitivity of this channel to deviations from the Standard Model with the energy. Scales for new physics in the range 250-750 GeV are excluded, depending on the type of coupling.

1 Introduction

Experiments at high energy colliders make it possible to probe previously untested sectors of the Standard Model, such as the vector boson self-interactions which depend only on the structure of the gauge group. The analysis described here probes the neutral sector of the gauge boson structure using the process $e^+e^- \to Z\gamma$. The couplings $ZZ\gamma$ and $Z\gamma\gamma$ vanish in the Standard Model at the lowest order, and higher order diagrams give very small contributions. Then, if new physics beyond the Standard Model is present in these couplings, $Z\gamma$ production provide a suitable framework to study it [1]. Previous limits on $ZZ\gamma$ and $Z\gamma\gamma$ couplings have been published at Fermilab [2] and at LEP [3].

The main experimental signature of the process $e^+e^- \to Z\gamma$ is the production of a photon of energy $E_\gamma = \frac{\sqrt{s}}{2}(1 - \frac{m_Z^2}{s})$, where $\sqrt{s}$ is the energy of the collision. Anomalous $ZZ\gamma$ and $Z\gamma\gamma$ couplings produce a global enhancement of the number of $Z\gamma$ events, and an enhancement of the number of longitudinally polarized Z bosons, which influences the angular distributions. In particular, an asymmetric polar angle distribution of the photon would be adirect signal of CP violation [1]. The anomalous couplings can be enhanced in compositeness models [4] or if new particles enter in higher order corrections.

In this analysis, the most sensitive channels, $e^+e^- \to q\bar{q}\gamma(\gamma)$ and $e^+e^- \to \nu\bar{\nu}\gamma(\gamma)$ are used to set limits on anomalous $ZZ\gamma$ and $Z\gamma\gamma$ couplings from the data taken by the L3 experiment [5] at LEP. These are the first limits which use the hadronic decays of the Z.

2 Event Selection

2.1 Selection of $e^+e^- \to q\bar{q}\gamma(\gamma)$ events

Events candidate to be $e^+e^- \to q\bar{q}\gamma(\gamma)$ are selected requiring high mulltiplicity, no energy imbalances, a neutral electromagnetic particle (photon) with its polar angle θ_γ in the range $14^\circ < \theta_\gamma < 166^\circ$ and an invariant mass of the system recoiling against the photon consistent with that of a Z: 80 GeV $< (s - 2E_\gamma\sqrt{s})^{1/2} <$ 110 GeV.

The number of selected events is 593 at all center-of-mass energies in the range 161-183 GeV. The acceptance of these cuts is estimated with the PYTHIA Standard Model $e^+e^- \to Z/\gamma^*\ \gamma \to q\bar{q}\gamma$ generator [6]. The generated events are required to lie in the fiducial region defined by the energy of the radiated photon greater than 20 GeV and its polar angle in the range $5^\circ < \theta_\gamma < 175^\circ$. Such events are passed through a simulation of the L3 detector response [7] and through the same analysis program used for data. The

$\sqrt{s}$(GeV)	Luminosity (pb^{-1})	Acceptance (%)	Events	Cross section (pb)
161	9.95	39.0 $\pm$ 0.7	117	30 $\pm$ 3
170	0.97	35.1 $\pm$ 0.7	7	21 $\pm$ 7
172	8.48	37.0 $\pm$ 0.7	59	19 $\pm$ 2
183	55.30	32.5 $\pm$ 0.3	410	22 $\pm$ 1

Table 1: Measured cross sections of the process $e^+e^- \to q\bar{q}\gamma(\gamma)$ at center-of-mass energies in the range 161-183 GeV. The PYTHIA $Z\gamma$ generator [6] is used in the determination of the acceptance.

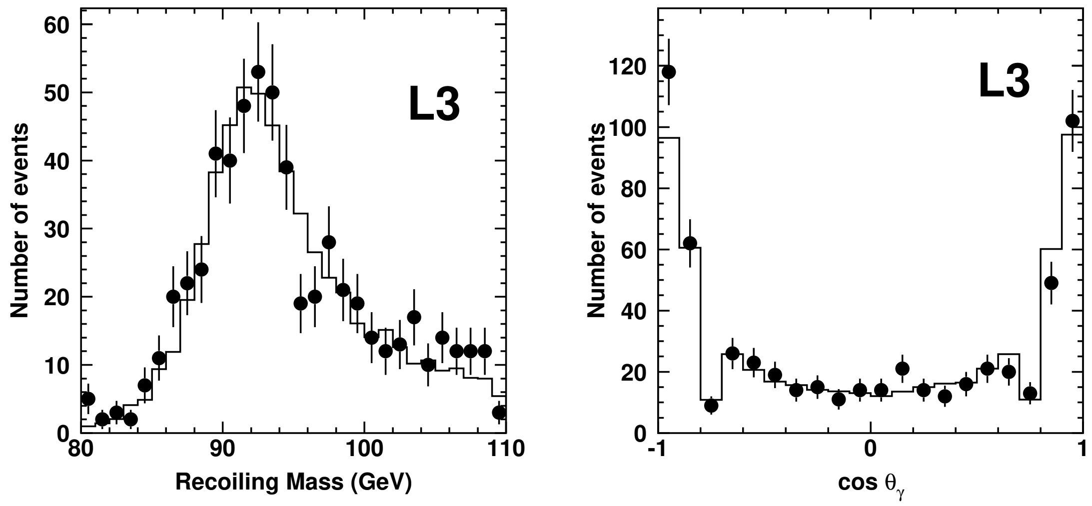

Figure 1: Distribution of the invariant mass of the system recoiling against the photon candidates (left) and Polar angle distribution of the photon candidates (right) in $e^+e^- \to q\bar{q}\gamma(\gamma)$ events. The mass is determined from the photon energy as $(s - 2E_\gamma\sqrt{s})^{1/2}$. Dots are data and the histogram is the Standard Model Monte Carlo prediction.

detector response as a function of time has been carefully taken into account. Due to the redundancy of multiplicity and energy triggers, the trigger inefficiency is estimated to be negligible.

The following backgrounds have been studied at the four center-of-mass energies: $e^+e^- \to W^+W^- \to qq\ \ell\nu$, $\ell = \mu, \tau$ [8] , which contributes with a negligible 0.019% to the data sample; and $e^+e^- \to q\bar{q}\ e\ \nu$ [9] , where the electron fakes a photon, mainly at low polar angles, giving 1.5% of background in the data sample. Using the measured luminosities, the number of selected events and the estimated acceptance in the fiducial region we obtain the cross sections (background substracted) shown in Table 1. They are in good agreement with the expectations from the Standard Model generator (28 pb at $\sqrt{s}$ = 161 GeV, 25 pb at $\sqrt{s}$ = 170 GeV, 23 pb at $\sqrt{s}$ = 172 GeV and 22 pb at

$\sqrt{s}$(GeV)	Luminosity (pb^{-1})	Acceptance (%)	Events	Cross section (pb)
161	10.32	28.6 $\pm$ 0.8	31	10.5 $\pm$ 2.2
170	0.99	28.3 $\pm$ 0.8	1	3.6 $\pm$ 2.6
172	8.79	28.8 $\pm$ 0.8	22	8.7 $\pm$ 2.1
183	52.55	32.0 $\pm$ 0.5	99	5.9 $\pm$ 0.6

Table 2: Measured cross sections of the process $e^+e^- \to \nu\bar{\nu}\gamma(\gamma)$ at center-of-mass energies in the range 161-183 GeV. The KORALZ $e^+e^- \to \nu\bar{\nu}\gamma(\gamma)$ generator [10] is used in the determination of the acceptance.

$\sqrt{s} = 183$ GeV).

Figure 1 shows the recoiling mass distribution and the polar angle of the photon candidates, respectively . Good agreement between data and Standard Model Monte Carlo is observed.

2.2 Selection of $e^+e^- \to \nu\bar{\nu}\gamma(\gamma)$ events

The candidate events for the $e^+e^- \to \nu\bar{\nu}\gamma(\gamma)$ channel are selected requiring very low multiplicity, a large total and transverse energy imbalance, an electromagnetic neutral particle (photon) in the range $16^\circ < \theta_\gamma < 164^\circ$, and an invariant mass of the system recoiling against the photon consistent with that of a Z: 80 GeV $< (s - 2\mathrm{E}_\gamma\sqrt{s})^{1/2} <$ 110 GeV.

A total of 153 events are selected at all center-of-mass energies in the range 161-183 GeV. The acceptance of these cuts is estimated with the KORALZ Standard Model $e^+e^- \to \nu\bar{\nu}\gamma(\gamma)$ generator [10]. All generated events which lie in the fiducial region defined in the previous section, are passed through a simulation of the L3 detector response [7] and through the same analysis program used for data. The detector response as a function of time has been carefully taken into account. The trigger efficiency is estimated to be above 99.7%.

The possible sources of background have been studied at the four center-of-mass energies: radiative bhabha events $e^+e^- \to e^+e^-\gamma(\gamma)$ [11, 12] ; and $e^+e^- \to WW \to e\ \nu_e l \nu_l$ [9], where the electron fakes a photon. No events passed the imposed cuts and therefore, we consider this channel as background free. Taking into account the measured luminosities, the number of selected events and the estimated acceptance in the fiducial region we obtain the cross sections shown in Table 2. They are in good agreement with the expectations from the Standard Model generator (8.2 pb at $\sqrt{s} = 161$ GeV, 7.0 pb at $\sqrt{s} = 170$ GeV, 6.9 pb at $\sqrt{s} = 172$ GeV and 5.5 pb at $\sqrt{s} = 183$ GeV). Figure 2 shows the recoiling mass distribution and the polar angle of the photon candidates. Good agreement between data and Standard Model Monte Carlo is observed.

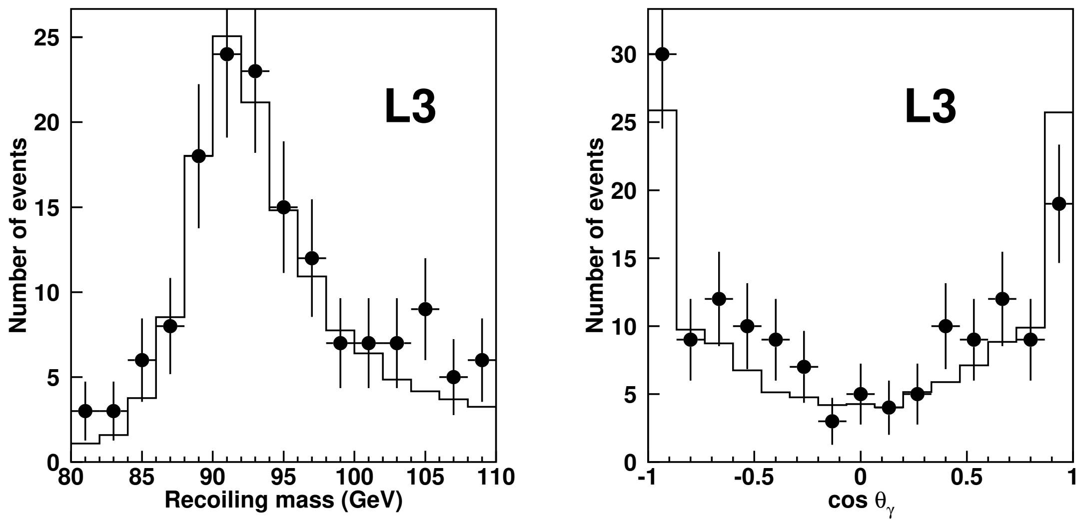

Figure 2: Distribution of the invariant mass of the system recoiling against the photon candidates (left) and Polar angle distribution of the photon candidates (right) in $e^+e^- \rightarrow \nu\bar{\nu}\gamma(\gamma)$ events. The mass is determined from the photon energy as $(s - 2E_\gamma\sqrt{s})^{1/2}$. Dots are data and the histogram is the Standard Model Monte Carlo prediction.

3 Limits on anomalous $ZZ\gamma$ and $Z\gamma\gamma$ couplings

3.1 Parametrization of the anomalous couplings and fits

Deviations from the Standard Model gauge structure are parametrized by means of four $ZZ\gamma$ and four $Z\gamma\gamma$ form factors h_i^V $(i = 1, 4; V = \gamma, \mathrm{Z})$, where a V superscript identifies a $\mathrm{Z}V\gamma$ anomalous coupling. The parameters h_1^V and h_2^V come from CP-violating amplitudes.

Each event is described using the following variables: the photon energy E_γ, its polar and azimuthal angles θ_γ, ϕ_γ, and the angles of the fermion f in the center-of-mass frame of the Z system: θ_f^{CM}, ϕ_f^{CM}. The Z system is defined by a boost back along the photon direction, with Lorentz factor $\gamma = m_Z/E_Z$.

We compute the amplitude for the process $e^+e^- \rightarrow f\bar{f}\gamma(\gamma)$ assuming Standard Model and Anomalous Couplings and taking into account the effects of the spin correlations, non-resonant contributions such as $e^+e^- \rightarrow \gamma^*\ \gamma \rightarrow f\bar{f}\gamma$ and the t-channel W-exchange corrections in $e^+e^- \rightarrow \nu_e\bar{\nu}_e\gamma$. Moreover, as a cross check, we have compared the results with those of the article from Baur and Berger [1], finding a perfect agreement in all cases.

Distributions in the presence of anomalous couplings can be obtained from the Standard Model ones by rewighting according to:

$$w(E_\gamma, \theta_\gamma, \phi_\gamma, \theta_f^{\rm CM}, \phi_f^{\rm CM}; h_i^V) = \frac{\mid (M_{\rm SM} + M_{\rm AC})(E_\gamma, \theta_\gamma, \phi_\gamma, \theta_f^{\rm CM}, \phi_f^{\rm CM}; h_i^V) \mid^2}{\mid M_{\rm SM}(E_\gamma, \theta_\gamma, \phi_\gamma, \theta_f^{\rm CM}, \phi_f^{\rm CM}) \mid^2} \tag{1}$$

For the $e^+e^- \to \nu\bar{\nu}\gamma(\gamma)$ case, the neutrino angular variables have been integrated out. On the other hand, we consider that additional photon radiation effects are small or cancel in the ratio of amplitudes. For the $e^+e^- \to q\bar{q}\gamma(\gamma)$ process, the angles $\theta_f^{\rm CM}$ and $\phi_f^{\rm CM}$ are substituted by the angles of the thrust axis in the Z center-of-mass frame, and the square of the amplitudes is symmetrized under the interchange $q \leftrightarrow \bar{q}$. The effect of this angle substitution is similar to the one studied in [13].

To determine the values of the anomalous couplings from the data, the following likelihood function is maximized:

$$\mathcal{L}(h_i^V) = \frac{N_t(h_i^V)^{N_o} \exp(-N_t(h_i^V))}{N_o!} \prod_{j=1}^{N_o} \frac{w_j(E_{\gamma j}, \theta_{\gamma j}, \phi_{\gamma j}, \theta_{fj}^{\rm CM}, \phi_{fj}^{\rm CM}; h_i^V)}{N_t(h_i^V)} \tag{2}$$

where, for each center-of-mass energy sample analyzed (161 GeV, 170 GeV, 172 GeV, 183 GeV), N_o is the number of observed events and $N_t(h_i^V)$ is the total number of expected events, determined by reweighting a very large sample at generator level and $w_j/N_t(h_i^V)$ is proportional to the probability density function of the event j. The proportionality factor is not included because it does not depend on the fitted variables h_i^V.

No additional smearing due to detector effects is applied to the five variables. The effect due to thia approximation is estimated using the Monte Carlo, by using the reconstructed values instead of the generated ones, and it is found to be very small compared to the statistical sensitvity. It is taken into account as a contribution to the systematic error.

The possible values for h_i^V are severely constrained by unitarity requirements and should vanish in the limit $s \to \infty$ [1, 14]. The usual choice for large values of s is [1, 2]:

$$h_i^V = \frac{h_{i0}^V}{(1+\frac{s}{\Lambda^2})^3}, i = 1,3 \qquad\qquad h_i^V = \frac{h_{i0}^V}{(1+\frac{s}{\Lambda^2})^4}, i = 2,4 \tag{3}$$

However, in e^+e^- colliders, the scale of new physics Λ must be above the energy of the collision $\sqrt{s}$. This energy is fixed, and therefore, no assumptions on the dependence of h_i^V form factors with the energy are needed. We can consider $h_i^V \equiv h_{i0}^V$ [15]. Anyway, we prefer another choice of the parameters to be fitted [1]:

$$\frac{\sqrt{\alpha}\, h_i^V}{m_Z^2} \equiv \frac{1}{\Lambda_{iV}^2}, i = 1,3 \qquad\qquad \frac{\sqrt{\alpha}\, h_i^V}{m_Z^4} \equiv \frac{1}{\Lambda_{iV}^4}, i = 2,4 \tag{4}$$

In these expressions the scales Λ_{iV} are naturally incorporated by the fact that h_1^V, h_3^V receive contributions from operators of dimension 6 and h_2^V, h_4^V are originated by operators of at least dimension 8 [15]. These scales have a more direct physical meaning, especially for future colliders, where h_i^V limits are expected to reach very small values.

3.2 Systematic errors and results

For the $\mathrm{q\bar{q}}\gamma$ channel, three sources of systematic errors are considered. The bias due to the use of reconstructed angles and energies in the likelihood fit is estimated to be below 0.02. Effects due to misidentification of the photon candidate are studied on a large Monte Carlo sample of $\mathrm{Z} \to \mathrm{q\bar{q}}$ events. It is found to be around 0.01. The contamination of $\mathrm{q\bar{q}}e\nu$ events is studied by introducing a 1.5% background on the Monte Carlo signal. It changes the fit results by 0.02.

Parameter	95% CL Limits ($\Lambda = 750$ GeV)	95% CL Limits (No Scale)
h_{10}^Z	$-0.60 < h_{10}^Z < 0.23$	$-0.50 < h_{10}^Z < 0.20$
h_{20}^Z	$-0.15 < h_{20}^Z < 0.43$	$-0.12 < h_{20}^Z < 0.34$
h_{30}^Z	$-0.57 < h_{30}^Z < 0.36$	$-0.48 < h_{30}^Z < 0.31$
h_{40}^Z	$-0.14 < h_{40}^Z < 0.48$	$-0.11 < h_{40}^Z < 0.38$
h_{10}^γ	$-0.28 < h_{10}^\gamma < 0.25$	$-0.23 < h_{10}^\gamma < 0.21$
h_{20}^γ	$-0.21 < h_{20}^\gamma < 0.22$	$-0.16 < h_{20}^\gamma < 0.17$
h_{30}^γ	$-0.37 < h_{30}^\gamma < 0.03$	$-0.31 < h_{30}^\gamma < 0.03$
h_{40}^γ	$-0.03 < h_{40}^\gamma < 0.28$	$-0.03 < h_{40}^\gamma < 0.22$

Table 3: Limits on the anomalous $\mathrm{ZZ}\gamma$ and $\mathrm{Z}\gamma\gamma$ couplings obtained by combining the processes $\mathrm{e^+e^-} \to \mathrm{q\bar{q}}\gamma(\gamma)$ and $\mathrm{e^+e^-} \to \nu\bar{\nu}\gamma(\gamma)$ at center-of-mass energies in the range 161-183 GeV at energy scales of 500 GeV and 750 GeV. In all fits, only one parameter is varied while the others are kept at zero.

Since no background or misidentification error can occur for the $\nu\bar{\nu}\gamma$ channel, the only bias is due to the use of the reconstructed photon variables, especially the energy. It is estimated to be below 0.02

Using the $q\bar{q}\gamma$ and $\nu\bar{\nu}\gamma$ samples altogether the limits in h_i^V summarized in Table 3 are obtained. We have also reformulated the likelihood function (2) using the parametrizations of formulae (4). The results are shown in Table 4.

Parameter	Fitted Value	95% CL Sensitivity
Λ_{1Z}	$\frac{1}{\Lambda_{1Z}^2} = (-0.21 \pm 0.19) \times 10^{-5}$	$\Lambda_{1Z} > 491$ GeV
Λ_{2Z}	$\frac{1}{\Lambda_{2Z}^4} = (+0.16 \pm 0.15) \times 10^{-9}$	$\Lambda_{2Z} > 248$ GeV
Λ_{3Z}	$\frac{1}{\Lambda_{3Z}^2} = (-0.16 \pm 0.22) \times 10^{-5}$	$\Lambda_{3Z} > 462$ GeV
Λ_{4Z}	$\frac{1}{\Lambda_{4Z}^4} = (+0.21 \pm 0.15) \times 10^{-9}$	$\Lambda_{4Z} > 249$ GeV
$\Lambda_{1\gamma}$	$\frac{1}{\Lambda_{1\gamma}^2} = (-0.00 \pm 0.13) \times 10^{-5}$	$\Lambda_{1\gamma} > 670$ GeV
$\Lambda_{2\gamma}$	$\frac{1}{\Lambda_{2\gamma}^4} = (-0.00 \pm 0.12) \times 10^{-9}$	$\Lambda_{2\gamma} > 262$ GeV
$\Lambda_{3\gamma}$	$\frac{1}{\Lambda_{3\gamma}^2} = (-0.17 \pm 0.09) \times 10^{-5}$	$\Lambda_{3\gamma} > 719$ GeV
$\Lambda_{4\gamma}$	$\frac{1}{\Lambda_{4\gamma}^4} = (+0.14 \pm 0.08) \times 10^{-9}$	$\Lambda_{4\gamma} > 290$ GeV

Table 4: Limits on new physics scales producing anomalous $ZZ\gamma$ and $Z\gamma\gamma$ couplings. Fitted values and limits are obtained by combining the processes $e^+e^- \to q\bar{q}\gamma(\gamma)$ and $e^+e^- \to \nu\bar{\nu}\gamma(\gamma)$ at center-of-mass energies in the range 161-183 GeV. In all fits, only one parameter is varied while the others are kept at zero.

While the "Fitted Value" column of Table 4 quantifies completely our sensitivity to new anomalous couplings, the 95% CL limits are definition dependent. A conventional approach is the one suggested in [16], in which the probability distribution is normalized over the physically allowed range of the parameters (that is, $\Lambda_{iV}^2 > 0, i = 1,3$; $\Lambda_{iV}^4 > 0, i = 2,4$), but even this approach is biased by the specific fitted value, despite of its consistency with the associated error. The "95% CL Sensitivity" column in Table 4 is the 95% CL limit that we should have obtained when fitting no anomalous effect at all. It has the advantage of being unbiased while reflecting our sensitivity in excluding new scales. There is no disadvantage for combination with other experiments, since only the fitted values and errors can be used for this purpose.

4 Conclusions

We have performed a search for anomalous $ZZ\gamma$ and $Z\gamma\gamma$ couplings at LEP2 using the $e^+e^- \to q\bar{q}\gamma(\gamma)$ and $e^+e^- \to \nu\bar{\nu}\gamma(\gamma)$ processes. No evidence of them has been found. This result can be quantified in a set of limits, the first ones obtained at LEP2 and the first limits which make use of hadronic decays of the Z. We exclude compositeness scales in the range 250-750 GeV, depending on the type of coupling.

These limits are comparable in sensitivity to the best present limits [2]. Since there is no need of energy-dependent form factors for e^+e^- colliders, our compositeness scale limits can be considered as independent of the coupling behaviour at energies larger than $\sqrt{s}$.

References

[1] F. M. Renard, Nucl. Phys. **B196** (1982) 93;
U. Baur, E. L. Berger, Phys. Rev. **D47** (1993) 4889;
P. Mery, M. Perrottet, F. M. Renard, Z. Phys. **C38** (1988) 579.

[2] F. Abe *et al.*, Phys. Rev. Lett. **74** (1995) 1941;
S. Abachi *et al.*, Phys. Rev. Lett. **79** (1997) 3640;
B. Abbott *et al.*, Fermilab-Pub-97/363-E (Submitted to Phys. Rev. Lett., October 1997).

[3] M. Acciarri *et al.*, Phys. Lett. **B 412** (1997) 201;
P. Abreu *et al.*, Phys. Lett. **B 380** (1996) 471.

[4] F.M. Renard, Phys. Lett. **B 126** (1983) 59;
M. Claudson, E. Farhi, R.L. Jaffe, Phys. Rev. **D 34** (1986) 873.

[5] B. Adeva *et al.*, Nucl. Inst. Meth. **A289** (1990) 35;
M. Acciarri *et al.*, Nucl. Inst. Meth. **A351** (1994) 300.

[6] T. Sjöstrand, CERN–TH/7112/93 (1993), revised August 1995;
T. Sjöstrand, Comp. Phys. Comm. **82** (1994) 74.

[7] The L3 detector simulation is based on GEANT Version 3.15.
R. Brun *et al.*, "GEANT 3", CERN–DD/EE/84–1 (Revised), 1987.
The GHEISHA program (H.Fesefeldt, RWTH Aachen Report PITHA 85/02 (1985)) is used to simulate hadronic interactions.

[8] M. Skrzypek, S. Jadach, W. Placzek and Z. Wąs, Comp. Phys. Comm. **94** (1996) 216;

M. Skrzypek, S. Jadach, M. Martinez, W. Placzek and Z. Wąs, Phys. Lett. **B 372** (1996) 289.

[9] F. A. Berends, R. Kleiss and R. Pittau, Nucl. Phys. **B 424** (1994) 308;
F. A. Berends, R. Kleiss and R. Pittau, Nucl. Phys. **B 426** (1994) 344;
F. A. Berends, R. Kleiss and R. Pittau, Nucl. Phys. (Proc. Suppl.) **B 37** (1994) 163;
R. Kleiss and R. Pittau, Comp. Phys. Comm. **83** (1994) 141;
R. Pittau, Phys. Lett. **B 335** (1994) 490.

[10] S. Jadach, B.F.L. Ward and Z. Wąs, Comp. Phys. Comm. **79** (1994) 503.

[11] J.H. Field, Phys. Lett. **B 323** (1994) 432;
J.H. Field and T. Riemann, Comp. Phys. Comm. **94** (1996) 53.

[12] D. Karlen, Nucl. Phys. **B 289** (1987) 23.

[13] The LEP Heavy Flavour Group, *QCD corrections to* $A_{\rm FB}^{\rm b\bar{b}}$ *and* $A_{\rm FB}^{\rm c\bar{c}}$ *Measurements at LEP1*, LEPHF/97-01, ALEPH 97-081 PHYSIC 97-071, DELPHI 97-131 PHYS 720, L3 Note 2154, OPAL Technical Note TN500, 18 August 1997.

[14] H. Czyz, K. Kołodziej, M. Krałek, Z. Phys. **C 43** (1989) 97.

[15] M. Suzuki, Phys. Lett. **153B** (1985) 289.

[16] R.M. Barnett *et al.*, *Review of Particle Properties*, Phys. Rev. **D 54** (1996) 1 and references therein.